Selected Features of the Character and Origins of Turbidity in the Catskill System

The Upstate Freshwater Institute

Syracuse, New York

10 January 2007

Background

During the Phase II Workshop on the Catskill Turbidity Control Study, given on August 24, 2006 at Kingston, NY, James Tierney, Watershed Inspector General and Assistant Attorney General, raised three questions concerning the character and origins of turbidity in the Catskill System that were not rigorously answerable within the material presented at that workshop. Reasonable representations of the questions are presented below:

1. Are there fundamental differences between the turbidity-causing particles from the Schoharie Reservoir discharge via the Shandaken Tunnel and those originating from along Esopus Creek and its watershed? Are particles from Schoharie Reservoir more "potent" with respect to turbidity or more persistent, compared to Esopus Creek particles?
2. What are the relative contributions of Esopus Creek (e.g., stream bank deposits) and Schoharie Reservoir (Shandaken Tunnel) to the turbidity load received by Ashokan Reservoir? What role does the Shandaken Tunnel input play in major events that require alum treatment?
3. What is the significance of using turbidity versus the total suspended solids metric to assess the issue of sources of turbidity for Ashokan Reservoir? Should we really be using turbidity?

These questions are addressed below, in the order as listed above, using an array of approaches and data sets.

A. The Extent of Heterogeneity in Features of Light Scattering (Turbidity) within the Catskill System (Question 1)

1. Introduction

Turbidity (Tn; NTU) is an optical measurement, representing a metric of the light scattered from a beam within a rather wide angle centered on 90° (Davies-Colley and Smith 2001). Light is scattered primarily as a result of its interaction with particles. Thus questions concerned with the heterogeneity of particles responsible for Tn in this and other systems are fundamentally problems in light scattering (intensity of this process represented by the scattering coefficient, $\boldsymbol{b}$). Measurements of Tn are known to be generally well correlated to $\boldsymbol{b}$, and other surrogates of $\boldsymbol{b}$ such as the beam attenuation coefficient ($\mathbf{c}$) at a wavelength of 660 nm ($\mathbf{c}_{660}$; Effler et al. 2006; $\lambda = 660$ nm minimizes the contribution of absorption to $\mathbf{c}$).

The magnitude of $\boldsymbol{b}$ (and therefore Tn) depends on four features of a particle population: (1) particle number concentration (N), (2) the particle size distribution (PSD), (3) particle composition, and (4) particle shape (Peng and Effler 2007). With appropriate characterizations of these features based on individual particles analysis, it would be possible to estimate $\boldsymbol{b}$ (at any specified λ; i.e., $\boldsymbol{b}(\lambda)$), and thereby partition the effects of the various factors, according to

$$\boldsymbol{b}(\lambda) = \sum_{i=1}^{N} Q_{\mathrm{b},i}(m_i, \lambda, d_i)\mathrm{PA}_i \qquad (1)$$

where $Q_{b,i}$ is the scattering efficiency of particle i with projected area PA_i. The value of $Q_{b,i}$ depends on the particle's relative (to water) refractive index ($m = n - in'$, where n and n' are the real and imaginary parts of the complex index of refraction, respectively), its size (d_i), and wavelength (λ). For inorganic particles, which dominate light scattering in the Catskill System, values of n depend on composition of particles, whereas those of n' are negligible (i.e., minimal light absorption). The application of Eq. (1) to estimate $\boldsymbol{b}$ from individual particles characteristics has been described as solving the forward problem in light scattering (Peng and Effler 2007).

Heretofore, resolution of the particle characteristics that regulate $\boldsymbol{b}$ (i.e., Tn) has been problematic. Bulk measurements of mass and mass fraction concentrations (disconnect with light scattering; e.g., Gelda and Effler 2007), and N and PSDs with particle counters all fail to provide the particle information necessary (Peng and Effler 2007) to address the light scattering problem implicit in the question raised relative to the heterogeneity of Tn-causing particles in the Catskill System. In sharp contrast to other measurements, scanning electron microscopy interfaced with automated X-ray microanalysis and image analysis (SAX) can directly assess N, PA_i, d_i, elemental X-ray composition (thus the geochemical type and m_i), and shape for large numbers of inorganic particles (Peng et al. 2002). This capability can support direct calculation of $\boldsymbol{b}$ [Eq. (1)]. Applications of SAX at Schoharie Reservoir (Peng and Effler 2007) have been successful in resolving the light-scattering features of inorganic (or minerogenic) particles, and achieving reasonably good closure with independent aggregate measures of $\boldsymbol{b}$.

It is valuable to consider the capabilities of SAX within the context of the question of the heterogeneity of turbidity-causing characteristics of particles within the Catskill System. Sources of heterogeneity in light scattering (turbidity) characteristics include particle composition (n), size distribution (d_i, PSD), and shape. Certain combinations of n and d_i, and shape could result in specified concentrations (N) of particles from a source (e.g., Schoharie Reservoir) yielding greater $\boldsymbol{b}$ (i.e., Tn) than the same N value from another source – consistent with the concept of differences in turbidity "potency". Moreover, greater contributions to $\boldsymbol{b}$ (i.e., Tn) from smaller particles in an upstream source (e.g., Schoharie Reservoir) of turbidity compared to another could result in greater persistence downstream in Ashokan Reservoir from the source of smaller particles. The approach to address these issues (Question 1 above) is to characterize and compare the features of light scattering through the Catskill System by SAX characterizations, specifically addressing: (1) particle composition, (2) PSD, and (3) particle shape.

2. Methods

a. SAX Protocols

SAX protocols, as adopted for the Catskill System, have been described in detail elsewhere (Peng et al. 2002; Peng and Effler 2007). Only selected features pertinent to this analysis are reviewed here. SAX provides both chemical (elemental X-ray counts) and morphometric characterizations of individual particles. Particles are compositionally classified into seven generic types – clay minerals, quartz, silica-rich, iron/manganese, miscellaneous (other minerogenic), diatoms, and organics (Table 1).

Morphometric characterization uses a "rotating chord" algorithm, which includes locating a centroid and specifying 16 chords through the centroid. The shape, or "nonsphericity", of a particle is represented by an aspect ratio (ASP)

$$ASP = D_{max} / D_{perp} \quad (2)$$

where D_{max} is the length of the longest chord through the centroid, and D_{perp} (or width) is the length of the chord perpendicular to D_{max} (i.e., ASP of a spherical particle is 1). PA_i is the sum of the areas of the triangles (defined by the centroid and series of chords). The value of d_i is calculated from PA_i assuming circular geometry.

Table 1. Specification of generic particle types, according to X-ray characteristics*.

Type	Description	X-ray characteristics	Sources/origins
Organics†	biological	low X-ray net counts (≤750)‡	autochthonous/ terrigenous
Clay	aluminosilicates	Al, 5–55%; Si, 20–85%; Al *plus* Si ≥ 50%	terrigenous
Si-rich	Si-containing minerals, silicates	60% ≤ Si < 90%	terrigenous
Quartz	mineral SiO_2	Si ≥ 90%, high X-ray density§	terrigenous
Fe/Mn	Fe/Mn-rich	Fe *plus* Mn ≥ 50%	autochthonous/ terrigenous
Diatom	biogenic SiO_2	Si ≥ 90%, low X-ray density§	autochthonous
Other**	miscellaneous particles	not specified	various

* X-ray characteristics refer to elemental X-ray relative intensities (in percentages).
† The 'Organics' component is a systematic underestimation of organic particles due to instrument limitation (Peng et al. 2002).
‡ Live X-ray acquisition time was 3 s.
§ The X-ray density in the 'Quartz' and 'Diatom' specifications refers to the ratio of a particle's total X-ray counts to its size (Peng et al. 2002).
** The 'Other' class incorporates all inorganic particles not captured in the specified classes.

b. Calculations of the Scattering Coefficient and Its Size Distribution

Values of $\boldsymbol{b}$ at $\lambda = 660$ nm were computed using Eq. (1) from SAX results. Values of $Q_{b,i}$ were calculated according to Mie theory for homogenous spheres (*also see* Peng and Effler 2007). Values of n were specified according to the generic classification results and literature values. The calculated contributions of various particle sizes to $\boldsymbol{b}$ (i.e., Tn) were represented in two formats, cumulative and non-cumulative contributions to the overall estimates of $\boldsymbol{b}$.

c. Brief System Description and Sampling Strategy to Address This Question

Sampling primarily focused on resolution of differences between contributions from Schoharie Reservoir and Esopus Creek, the two distinguishable sources that influence downstream turbidity conditions. Samples collected from eight locations within the Catskill System, extending from Schoharie Reservoir into Kensico Reservoir, were analyzed to

characterize and compare light-scattering features of particles. These sites included (Figure 1) the Schoharie Reservoir withdrawal, Esopus Creek upstream (above portal, AP) and downstream (E16i/Coldbrook) of the Shandaken discharge, the west basin of Ashokan Reservoir proximate to the weir (DEP Limnology site 3), the east basin of Ashokan Reservoir proximate to the intake (sent to Kensico, DEP Limnology site 4), and two sites in the Catskill arm of Kensico Reservoir (DEP Limnology sites 4.1 and 4.2). The sampling and analyses presented here focused on 2005, a particularly severe case for the turbidity issue in the Catskill System. Summary findings for Schoharie Reservoir in 2002 (Peng and Effler 2007) are also included for comparison. A total of 30 samples collected in 2005 were analyzed with SAX to support this evaluation.

A wide range of runoff, and therefore Tn levels (e.g., O'Donnell and Effler 2006), is represented in the sampling program (Table 2). Additionally, samples collected downstream of the discharge (Shandaken Tunnel) included cases when the tunnel was on and when it was off (Table 2). Accordingly, contributions from Schoharie Reservoir in Esopus Creek are included for cases with the tunnel on, and excluded for cases with the tunnel off.

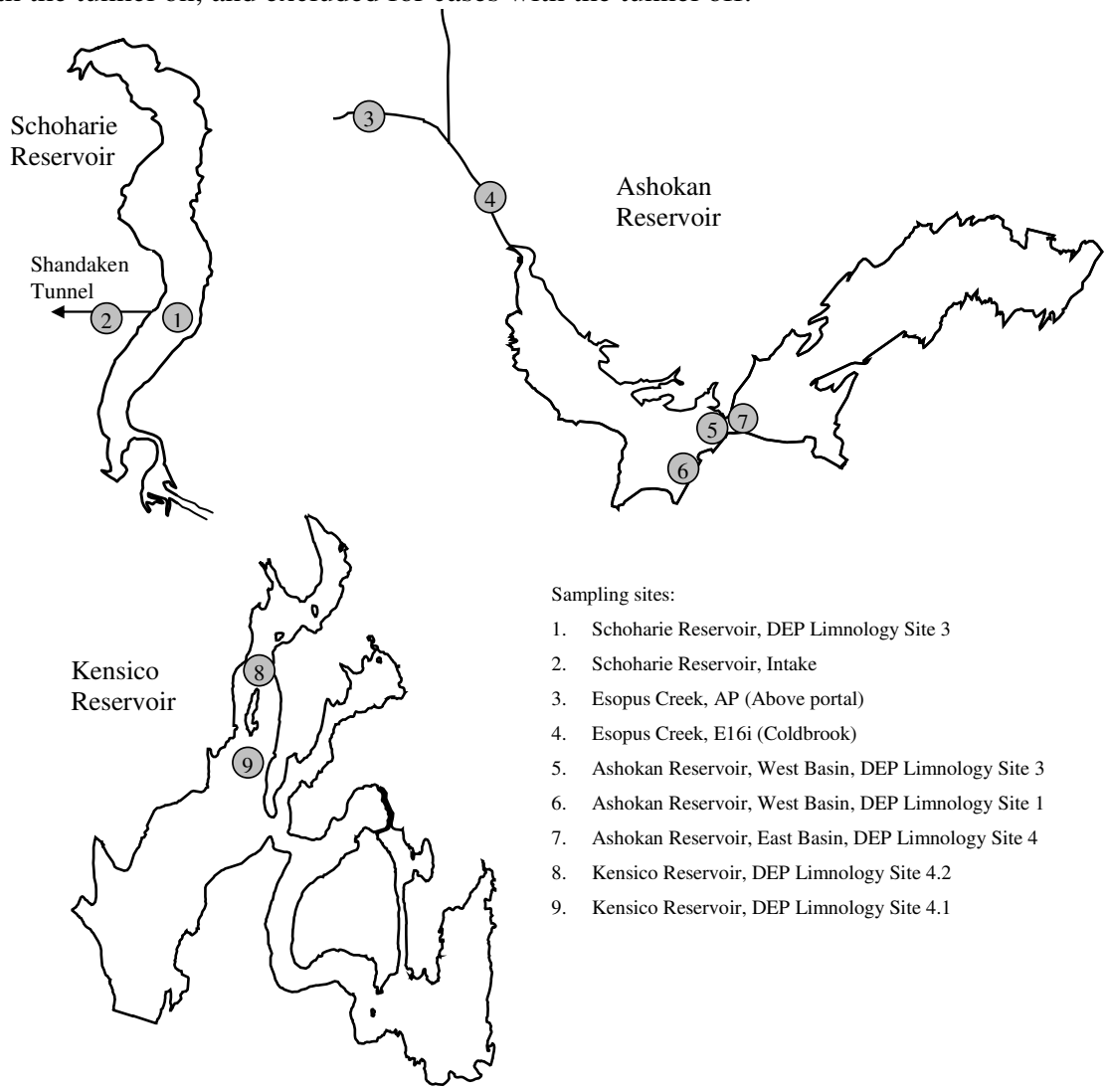

Figure 1. SAX sampling sites.

Table 2. Sample (2005) characteristics and SAX results.

Waterbody	Site / Depth	Date	Tn	PAV*	Tunnel	d_{50}*	mean	PAV Type Composition (%)				
			(NTU)	($cm^2\ L^{-1}$)		(μm)	ASP*	Clay	Quartz	Si-rich	Fe/Mn	Misc
Schoharie Res.	Intake	Apr 7	440	856.8		2.43	1.89	69.8	16.7	5.0	1.0	2.4
	3 / 15 m	Apr 7	434	843.9		2.54	1.88	74.7	14.8	3.8	1.7	2.6
	3 / 10 m	Jun 21	7.2	10.64		5.21	2.27	87.9	5.0	2.3	0.5	1.3
	3 / 10 m	Jul 6	4.6	7.13		3.95	2.01	80.4	10.9	3.1	0.9	2.4
	3 / 10 m	Jul 19	2.2	3.72		6.06	2.58	90.2	1.7	3.1	0.6	2.3
	3 / 10 m	Aug 2	4.3	14.94		6.51	2.43	92.1	3.5	1.0	0.3	0.9
	3 / 10 m	Aug 17	3.2	8.47		5.76	2.40	93.6	1.8	2.0	0.6	0.9
	3 / 10 m	Aug 30	6.9	14.98		5.04	2.17	87.9	4.8	1.6	0.9	1.3
	3 / 10 m	Sep 14	27.8	65.02		5.13	2.12	84.2	6.9	1.7	1.4	1.8
Esopus Creek	AP	Jan 11	1.5	3.19	off	2.33	2.00	71.0	11.1	3.8	1.0	10.4
	AP	Jan 11	1.6	3.00	off	2.55	1.92	70.4	12.8	4.8	1.6	3.6
	AP	Feb 22	2.3	4.68	on	2.53	1.93	76.6	11.9	3.9	1.0	3.9
	AP	Feb 22	1.7	4.11	on	2.35	1.97	76.0	10.2	6.7	0.9	1.8
	AP	Apr 13	76.1	188.2	off	2.74	1.82	76.6	15.2	1.9	0.7	2.4
	AP	Jul 19	18.8	35.45	on	2.88	1.78	71.3	7.0	7.2	1.3	4.2
	E16i	Jan 11	2.6	4.10	off	2.46	1.90	73.0	15.7	4.4	1.2	3.1
	E16i	Feb 22	5.6	7.45	on	2.24	1.86	75.8	12.5	3.5	1.9	2.7
	E16i	Apr 13	66.7	192.5	off	2.66	1.88	70.5	15.3	4.2	0.7	3.7
	E16i	Jul 19	23	41.72	on	2.86	1.83	82.9	6.5	6.3	0.5	1.6
Ashokan Res. W.	1 / 3 m	Apr 4	94.2	387.8	off	2.39	1.97	77.1	14.4	4.2	1.0	1.8
	1 / 6 m	Apr 4	242	721.6	off	2.76	1.79	73.8	18.0	4.5	0.8	1.6
	1 / 32 m	Apr 4	464	1380.2	off	1.81	2.08	78.5	12.7	3.0	1.8	2.3
	3 / 2 m	Apr 5	231	640.6	off	2.80	1.90	75.9	14.5	3.5	0.8	2.5
	3 / 0 m	Jul 7	3.7	3.95	on	2.91	1.99	75.9	9.9	7.5	0.6	2.9
	3 / 0 m	Aug 17	1.7	2.97	on	2.75	2.49	75.2	9.8	7.1	1.0	1.1
Ashokan Res. E.	4 / 2 m	Apr 7	31.8	67.18		2.61	1.83	67.1	20.7	4.5	1.5	3.5
	4 / 0 m	Jul 7	2.57	4.47		3.09	2.14	84.1	4.8	5.0	0.4	1.9
Kensico Res.	4.2 / 10 m	Apr 6	21.5	60.95		2.84	1.82	74.1	17.1	3.0	0.8	2.0
	4.1 / 10 m	May 17	1.57	3.35		2.79	2.88	78.3	5.4	6.2	1.8	2.0

*PAV, d_{50}, and ASP – defined subsequently

3. Results

a. Composition of Minerogenic Particles in Catskill System

Chemical composition results are presented in the form of percent (%) contributions of the particle types to overall sample PA per unit volume (PAV), a primary regulator of $\boldsymbol{b}$ [i.e., Tn; *see* Eq. (1)]. The chemical classification scheme, based on elemental X-ray relative intensities (Table 1), performed well in representing the minerogenic particles of the Catskill System, as more than 95% of the total PAV was in the specified particle types (i.e., not in miscellaneous group). Averaged composition information for the various study sites is presented in Table 3. Results for 2002 in Schoharie Reservoir, based on a larger number of samples, are included for comparison.

The primary features of the particle composition results are (Table 3): (1) the relative uniformity of the chemical composition of the turbidity-causing particle populations throughout the Catskill System, extending through the Catskill arm of Kensico Reservoir, and (2) the dominance of clay mineral particles in these particle assemblages. This uniformity is particularly strong outside of Schoharie Reservoir, where a somewhat larger contribution by clay particles and smaller contribution by quartz was observed.

Table 3. Summary of PAV magnitude and composition (mean ± standard deviation) of particle populations through the Catskill System. Samples were collected in 2005 unless otherwise noted.

Sites		Number of Samples	Tn range	PAV range	Type distribution (%)				
			(NTU)	($cm^2 L^{-1}$)	Clay	Quartz	Si-rich	Fe/Mn	Other
Schoharie	2002	53	4.2–81	9.8–199.3	79.4 ± 3.8	7.7 ± 2.7	3.6 ± 1.1	1.5 ± 0.7	3.4 ± 1.7
	2005	9	2.2–440	3.7–856.8	84.5 ± 8.1	7.3 ± 5.5	2.6 ± 1.2	0.9 ± 0.4	1.8 ± 0.7
Esopus AP		6	1.5–76	3.0–188	73.7 ± 3.0	11.4 ± 2.7	4.7 ± 2.0	1.1 ± 0.3	4.4 ± 3.1
Esopus E16i		4	2.7–67	3.3–192	75.5 ± 5.3	12.5 ± 4.2	4.6 ± 1.2	1.1 ± 0.6	2.8 ± 0.9
Ashokan West Basin		6	1.7–464	3.0–1380	76.1 ± 1.6	13.2 ± 3.1	5.0 ± 1.9	1.0 ± 0.4	2.0 ± 0.7
Ashokan East Basin		2	2.6–31.8	4.5–125	75.6 ± *	12.7 ± *	4.7 ± *	0.9 ± *	2.7 ± *
Kensico		2	1.6–22	3.4–61	76.2 ± *	11.2 ± *	4.6 ± *	1.3 ± *	2.0 ± *

* only two observations, standard deviation not reported.

b. Shapes of Minerogenic Particles in Catskill System

The extent of deviations of minerogenic particle shapes from sphericity for the various sites of the study is described by average ASP values (Table 4). The primary feature of these results is the uniformity in the extent of nonsphericity of the particle populations throughout the Catskill System, indicating a similarity of the distribution of particle shapes for these assemblages. The magnitude of deviations from sphericity (ASP = 1) is consistent with the "plate-like" structure of many of the clay mineral particles observed, and is similar to conditions reported earlier for Schoharie Reservoir (Peng and Effler 2007)

Table 4. Particle Shapes (aspect ratio, ASP; mean ± standard deviation) for sites through the Catskill System. Samples were collected in 2005 unless otherwise noted.

Sites		Number of Samples	ASP
Schoharie	2002	53	1.75 ± 0.09*
	2005	9	2.19 ± 0.20
Esopus AP		6	1.90 ± 0.08
Esopus E16i		4	1.87 ± 0.03
Ashokan West Basin		6	2.03 ± 0.2
Ashokan East Basin		2	1.98 †
Kensico		2	2.35 †

* 'Clay'-type particles only (Peng and Effler 2007).
† only two observations, standard deviation not reported .

c. Size Contributions of Minerogenic Particles to $\boldsymbol{b}$ (i.e., Tn) in Catskill System

The contributions of various sizes of minerogenic particles to calculated values of $\boldsymbol{b}$ at λ = 660 nm ($\boldsymbol{b}_{660}$) for a sample collected from the E16i site on Esopus Creek on April 13, 2005 (where Tn = 66.7 NTU) are presented in both the cumulative and non-cumulative formats in Figure 2. The results are also presented in the form of percent of the estimated total $\boldsymbol{b}_{660}$ value (*see* Y-axes on the right). According to these calculated patterns, the vast majority of $\boldsymbol{b}$ (i.e., Tn) is associated with particles in the size range 1–10 μm (Figure 2). A peak contribution was made by particles slightly larger than 2 μm in this sample, with a secondary maximum for particles slightly larger than 4 μm (Figure 2b). These size dependency patterns were generally recurring for the samples analyzed in this study. A valuable simplifying statistic to represent the size dependency characteristics of $\boldsymbol{b}$ for the samples is identified here, d_{50}, the fifty percentile (i.e., median) size. Accordingly, half of the total $\boldsymbol{b}$ is associated with particles smaller than d_{50}, the other half is attributable to those larger than d_{50}.

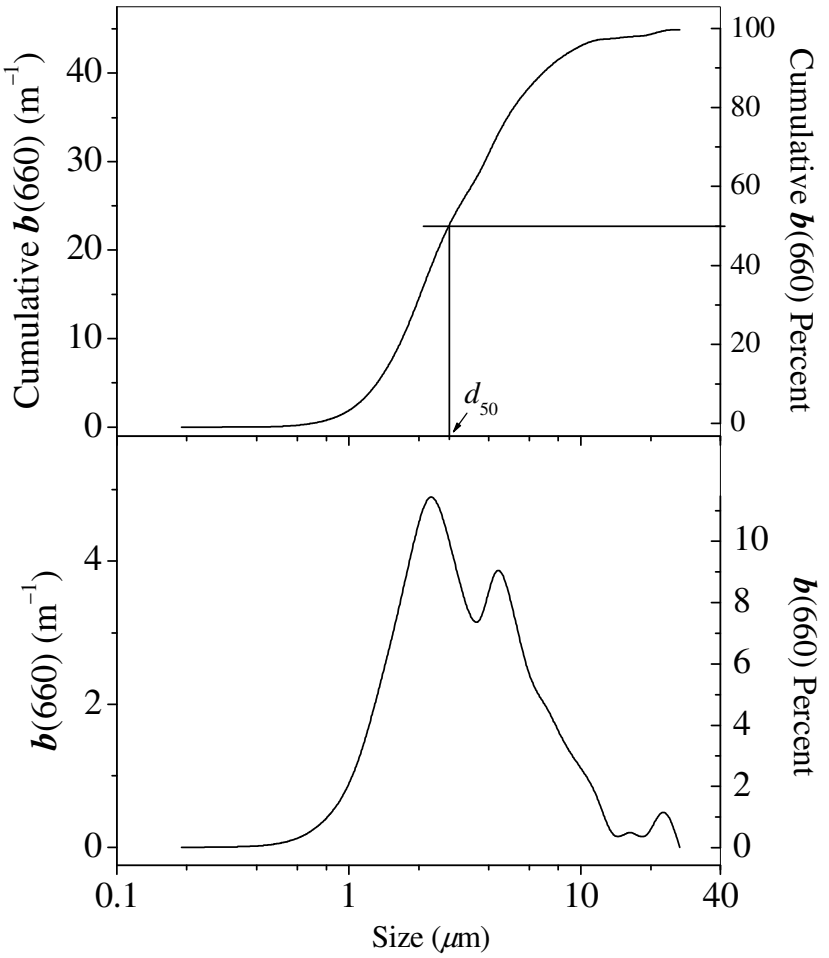

Figure 2. Particle size contributions to total b_{660}: (a) cumulative, and (b) non-cumulative. Sample was collected at site E16i on April 13, 2005 (Tn 66.7 NTU; Shandaken tunnel off).

Cumulative contributions to ***b*** patterns for samples from four sites are presented for elevated runoff conditions in 2005 that depict a high degree of similarity (Figure 3) for the Schoharie Reservoir water column adjoining the intake, water exiting Schoharie Reservoir, and both upstream (AP), and downstream (E16i) of the tunnel input in Esopus Creek. A shift of minor magnitude to higher d_{50} values in the stream relative to Schoharie Reservoir was observed. Very similar patterns (and d_{50} values, Figure 3) for the upstream (AP) and downstream (E16i) sites on Esopus Creek were again observed on April 13, 2005, when the tunnel had been turned off.

The spatial pattern of d_{50} amongst the study sites during the elevated runoff conditions of 2005 demonstrated a high degree of uniformity (Figure 4), despite wide differences in the Tn level amongst the sites. Values of d_{50} were in the narrow range of 2.4–2.9 μm, despite Tn values that ranged from 21.5 NTU (Kensico Reservoir, site 4.2, 10 m, 4/6/2005) to >400 NTU in Schoharie Reservoir.

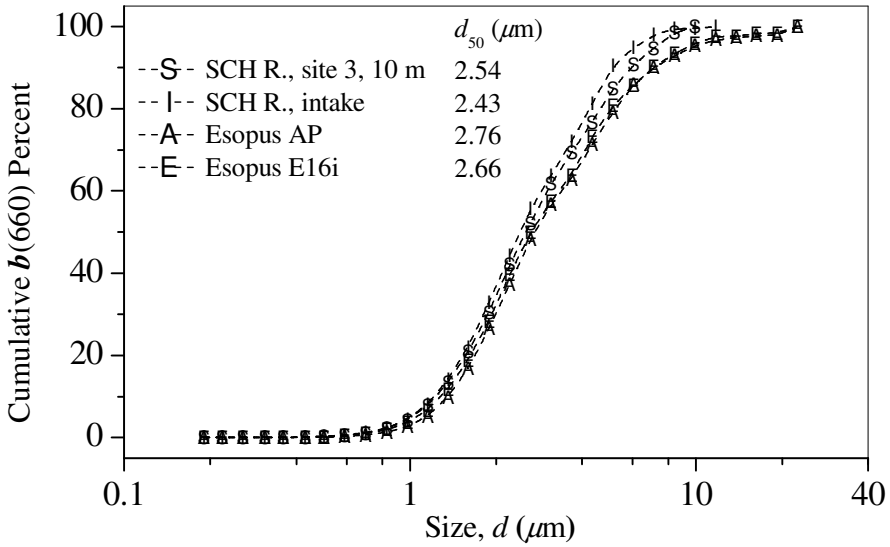

Figure 3. Cumulative percent contributions to total b_{660} for four samples collected during April 2005 storm event; values of d_{50} were identified . Samples from site 3 and intake of Schoharie Reservoir were collected on April 7 (turbidities 434 and 440 NTU, respectively), those from AP and E16i on April 13 (turbidities 76.1 and 66.7 NTU, respectively; Shandaken tunnel off)

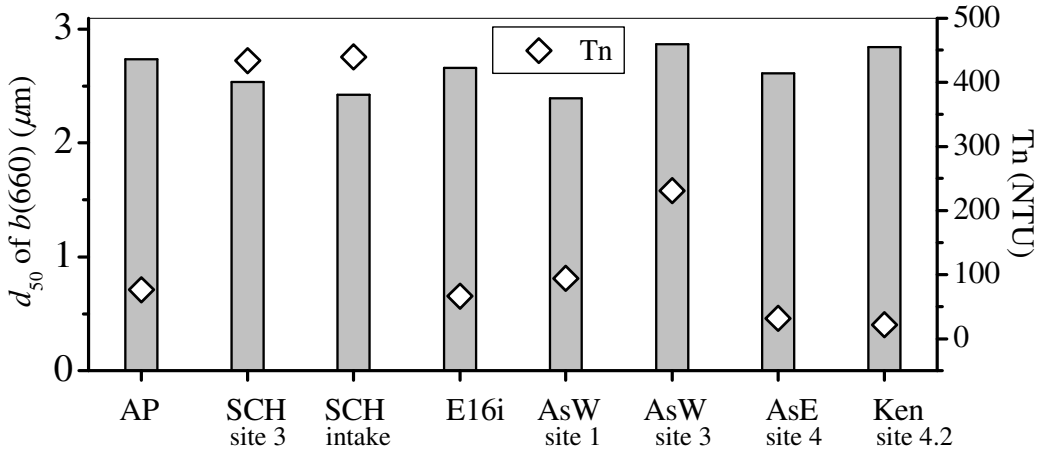

Figure 4. Median sizes of b_{660}, d_{50}, and turbidities for samples collected during April 2005 storm event. Sample details (site number correspond to DEP Limnology designations):

AP—Esopus Creek, upstream (above portal), 4/13/05;
SCH Sta3—Schoharie Reservoir, site 3, 10 m, 4/7/05;
SCH Intake—Schoharie Reservoir, water withdrawal, 4/7/05;
AP—Esopus Creek, upstream (above portal), 4/13/05;
E16i—Esopus Creek, downstream (Coldbrook), 4/13/05;
AsW Sta1—Ashokan Reservoir, W. basin, site 1, 3 m, 4/4/05;
AsW Sta3—Ashokan Reservoir, W. basin, site 3, 2 m, 4/5/05;
AsE Sta4—Ashokan Reservoir, E. basin, site 4, 2 m, 4/7/05;
Ken Sta4.2—Kensico Reservoir, site 4.2, 10 m, 4/6/05.

The average d_{50} values for the study sites are presented in Table 5 (*see also* Table 2), that support the general uniformity of size contributions to $\boldsymbol{b}$ (i.e., Tn) within the Catskill System extending downstream into the corresponding arm of Kensico Reservoir. Average d_{50} values ranged from 2.6 to 5.4 μm. Note two sets of results are presented for Schoharie Reservoir, one for during and immediately following the major April runoff event, the other for rest of the samplings of 2005. The higher values observed two months after the major runoff event probably reflect the effects of sediment resuspension associated with rapid drawdown during that interval.

Table 5. Average median size (d_{50}) of scattering ($\boldsymbol{b}_{660}$) (mean ± standard deviation) for sites through the Catskill System. Samples were collected in 2005.

Sites		Number of Samples	d_{50} (μm)
Schoharie	Apr 7	2	2.48 *
	Jun–Sep	7	5.38 ± 0.83
Esopus AP		6	2.56 ± 0.22
Esopus E16i		4	2.56 ± 0.27
Ashokan West Basin		6	2.57 ± 0.41
Ashokan East Basin		2	2.85 *
Kensico		2	2.82 *

* only two observations, standard deviation not reported

d. Evidence of Closure for Estimates of $\boldsymbol{b}$

Two forms of closure of SAX measures and corresponding estimates $\boldsymbol{b}$ with Tn observations for the study sites are presented in support of the representativeness of the overall analysis: (1) an evaluation of the relationship between the aggregate Tn measurements and PAV determinations by SAX (Figure 5a), and (2) an evaluation of the relationship between Tn and calculated $\boldsymbol{b}_{660}$ (Figure 5b). Both relationships were quite strong, especially when considered over a smaller portion of the large range encountered in the study, supporting the veracity of the SAX measurements as well as the calculation of minerogenic $\boldsymbol{b}$. The similarity in the two relationships (Figure 5a and b) depicts the dominant role PA_i determinations (i.e., PAV) play in the estimates of $\boldsymbol{b}$, and thereby the uniformity of effective scattering efficiency factors ($<Q_b>$; ratio of $\boldsymbol{b}$ to PAV) for the Catskill System (Eq.(1)). The uniformity of $<Q_b>$ is consistent with the above reported uniformity in the chemical composition and d_{50} (i.e., PSD) of the turbidity-causing minerogenic particle populations within the Catskill System and extending into the corresponding arm of Kensico Reservoir.

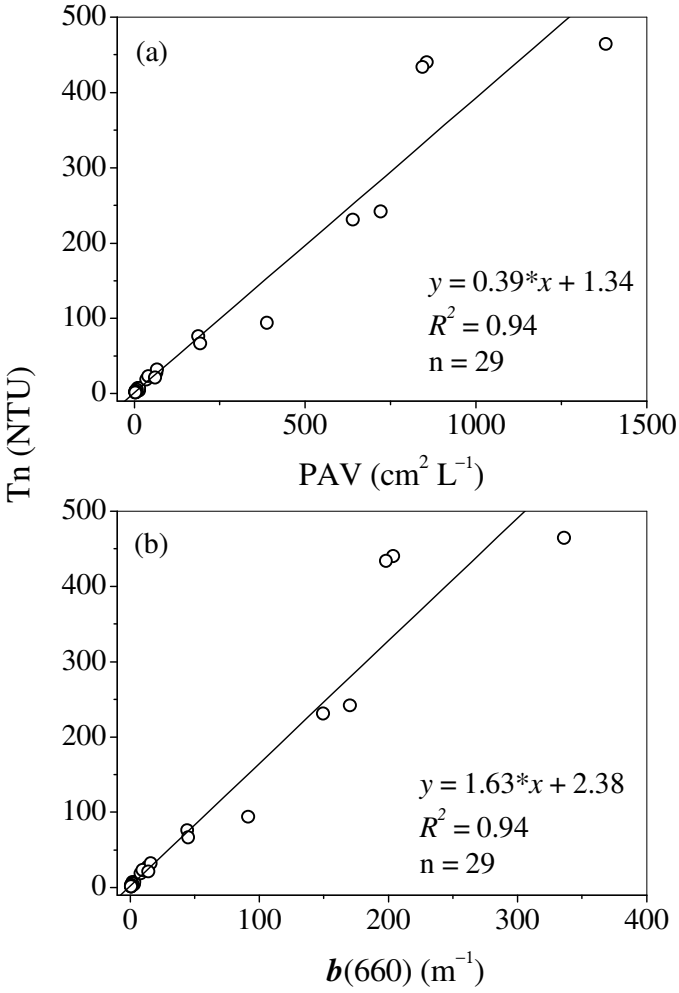

Figure 5. Evaluation of the relationships between turbidity and SAX measurements and estimates: (a) PAV, and (b) b_{660}. Samples were collected in 2005.

4. Discussion and Implications of Results

Mobilization of particles during intervals of elevated runoff associated with high turbulence and imparted shear stress is a well recognized phenomenon that widely results in increased concentrations of suspended solids and turbidity. Further, shifts to greater contributions by larger sized particles to particle populations during such events are also acknowledged. However, the associated effects on the character of the turbidity-causing portion of the particle populations have generally not been accessible based on commonly used particle characterization technologies. SAX has provided resolution of this issue for the Catskill System, where minerogenic particles regulate Tn levels.

The SAX measurements presented here provided definitive information on these issues and concerns with respect to potential differences in "potency" and persistence of turbidity-causing particles within the Catskill System. First, minerogenic particles over the size range 1–10 μm regulate turbidity throughout this system over wide ranges of runoff and associated Tn levels. Moreover, the composition of minerogenic particles, the relative contribution of particle sizes (within the 1–10 μm range) to turbidity, and particle nonsphericity remain relatively uniform within the Catskill System over a wide range of runoff conditions and Tn levels. These results provide strong support for not invoking differences in "potency" and "persistence" of turbidity within the Catskill System. Specifically, the hypothesis that the turbidity from Schoharie Reservoir is substantially different from or more problematic than other portions of the Catskill System (e.g., Esopus Creek) is not supported based on characterization of the light scattering properties of the particle population of the system.

These findings should not be interpreted as indications that there are no noteworthy temporal and spatial differences in particle populations within the Catskill System. In particular, we expect differences and dynamics in particle sizes related to the differences in lentic (i.e., reservoir) and lotic (stream) environments and in response to runoff events, that are expected to be manifested in larger sizes not critical to $\boldsymbol{b}$ (likewise, Tn). These factors should be expected to contribute to spatial and temporal differences in the relationship between gravimetric (e.g., TSS) and optic (e.g., Tn) metrics of particle populations.

B. Turbidity Loadings from Schoharie Reservoir Discharge and Esopus Watershed into Ashokan Reservoir (Question 2)

1. Introduction

Esopus Creek is the primary tributary of Ashokan Reservoir that carries suspended material from its watershed and from the Schoharie Reservoir discharge (Shandaken Tunnel). Elevated turbidity (T_n) levels are known to occur in Esopus Creek during runoff events, even during intervals when the tunnel is not discharging. The turbidity of the water discharged from Schoharie Reservoir can vary seasonally and year-to-year, depending upon the operation of the reservoir and runoff events in its own watershed. Thus, the turbidity of the water entering Ashokan Reservoir depends upon the flow rate and turbidity of both the tunnel and Esopus Creek (e.g., stream banks) sources. Here the relative importance of each of these sources of turbidity is quantified.

Locations of various monitoring sites in the watershed are shown in Figure 6. Site SRR2 is located at the end of Shandaken Tunnel just before it meets Esopus Creek. Site E16i is proximate to the mouth of Esopus Creek where it enters Ashokan Reservoir. The flow and turbidity monitored at E16i reflect contributions from both the tunnel and Esopus watershed.

Turbidity, while an optical property, behaves as an intensive property, just like concentration of any other water quality constituent due to the additive character of its sources and components. This behavior allows us to perform mass balance type calculations for turbidity and to estimate turbidity (quasi-) loads (Davies-Colley et al. 1993).

2. Calculations and Support Data

Hourly turbidity loading was computed by simply multiplying turbidity by the flow rate:

$$\text{Turbidity Load (NTU}\cdot\text{m}^3\text{)} = \text{Turbidity (NTU)} \cdot \text{Flow (m}^3\text{/s)} \cdot 3600 \qquad (3)$$

Annual turbidity load was obtained by summing hourly values.

Table 6 lists the data used in this analysis. Sites EAR and CATALUM are located in the Catskill Aqueduct that flows into Kensico Reservoir at the points of withdrawal from Ashokan Reservoir and at the point of entry into Kensico Reservoir (Figure 6). Flow is monitored continuously at both SRR2 and E16i sites, while turbidity is monitored rather less frequently.

3. Results and Discussion

The analysis of the data is divided into two parts. In the first part, turbidity loads are estimated for 1991-2005 using a flow-turbidity relationship developed with less frequent measurements made by DEP. In the second part, turbidity patterns observed in Esopus Creek and Shandaken Tunnel discharge are documented for 2005 – the year of most comprehensive measurements of turbidity at E16i.

Table 6. Data used for turbidity loading calculations.

Parameter	Location	Duration	Frequency	Source	Notes
Flow	SRR2	1991-1997	Daily	DEP	linearly interpolated to get hourly data
	SRR2	1998-2005	Hourly	USGS	USGS
	E16i	1991-2005	Hourly	USGS/DEP	1991-1997 from DEP
Turbidity	SRR2	1991-2005	~5/week	DEP	linearly interpolated to get hourly data
	E16i	1995-2005	~5/week routine	DEP	limited storm events data included
	E16i	2005	15-min	UFI	missing data filled with flow-turbidity regressions, when tunnel is off
	EAR	1991-2005	~5/week	DEP	
	CATALUM	1991-2005	~5/week	DEP	

Figure 6. Esopus Creek watershed, location of diversion from Schoharie Reservoir (SRR2), sampling station at the mouth of Esopus Creek (E16i), and Catskill Aqueduct (EAR and CATALUM).

a. Turbidity input to Ashokan Reservoir for 1991-2005:

Most of the turbidity load from the Esopus watershed is delivered during short duration runoff events. However, not all events were monitored at E16i at the desirable frequency of at least once every hour during the study period of 1991-2005. Therefore, in order to estimate and partition contributions between the tunnel and the Esopus Creek watershed turbidity loadings we developed a flow-turbidity relationship from the less frequent routine and storm monitoring data of DEP, to specify values for intervals when observations were not available. Further, adjustments must be made for contributions of the tunnel. To develop a flow-turbidity relationship, we used paired instantaneous flow (interpolated from hourly flow) and turbidity at E16i when the Shandaken Tunnel was not operating ($Q < 0.17$ m^3/s) for 1995-2005. This isolates Esopus Creek characteristics from the effects of turbidity additions from the tunnel. Data recorded prior to 1995 could not be used because there was no information available regarding time of sample collection.

A nonlinear relationship ($r^2 = 0.62$) was obtained between flow and turbidity at E16i (Figure 7). While there is significant scatter in this, it represents a reasonable approach for our analysis of partitioning of turbidity loading from the two sources. A portion of the scatter can be explained by examining observations of flow and turbidity for some of the runoff events in the watershed. For example, huge runoff events in January 1996 and April 2005 eroded parts of stream banks which resulted in continual sources of turbidity-causing particles (Figure 8). Thus, prolonged elevated turbidity levels following large runoff events are observed at E16i (Figure 8). We did not see any improvement in the flow-turbidity relationship when rising and falling limbs of the storms data (from detailed monitoring in 2005) were considered separately.

Hourly turbidity concentrations were generated using this relationship from hourly flows for 1991-2005. Finally, the Esopus Creek watershed loads were computed by multiplying flow and turbidity. Turbidity at SRR2 was linearly interpolated to obtain hourly values. Large diurnal variations in turbidity at SRR2 are not expected as Schoharie Reservoir would have modulated the events. Furthermore, during major events, no discharge is made from the reservoir.

A comparison of the total annual load from the tunnel versus the watershed is depicted in Figure 9. Substantial interannual variation is observed in the estimates of turbidity loading from the watershed which is associated with the runoff volume (cv = 194%). In contrast, it is less variable from the tunnel (cv = 68%). Further, on average (for the study period), the tunnel contributes only 2% of the total turbidity load. Relative to the total load, the highest contribution from the tunnel (43%) was observed in 2001 (Table 7), though the magnitude of the total load was the fourth smallest in that year (Figure 9). The absolute magnitude of the loading from the tunnel was the highest; approximately three times the average loading, in 2005 (Figure 9). It should be noted that in 2005 Schoharie Tunnel diversion was operated beyond normal water supply needs to keep the reservoir drawndown to facilitate maintenance work at Gilboa Dam.

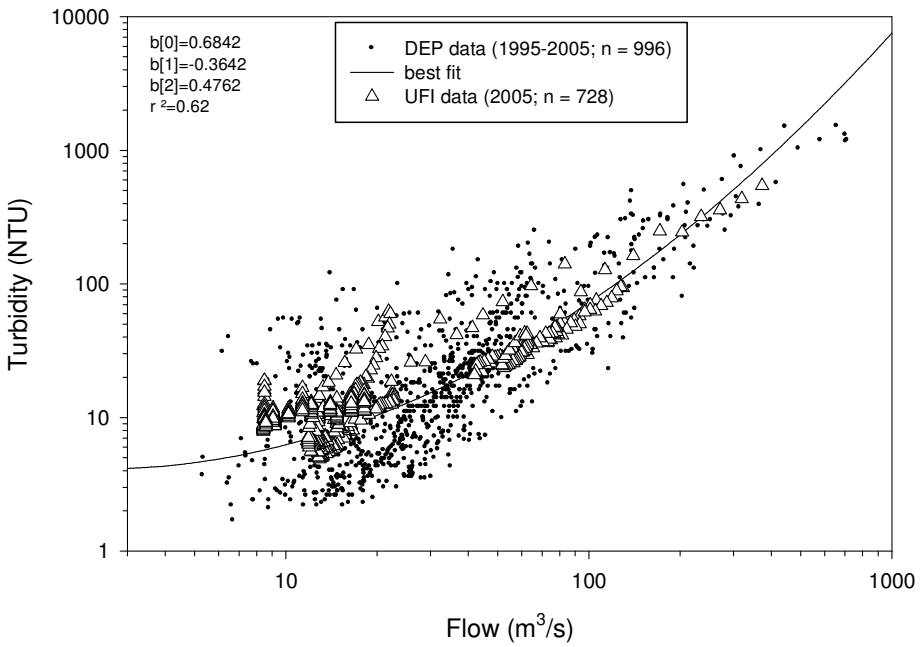

Figure 7. Flow-turbidity relationship for site E16i when the Schoharie diversion tunnel was not in use.

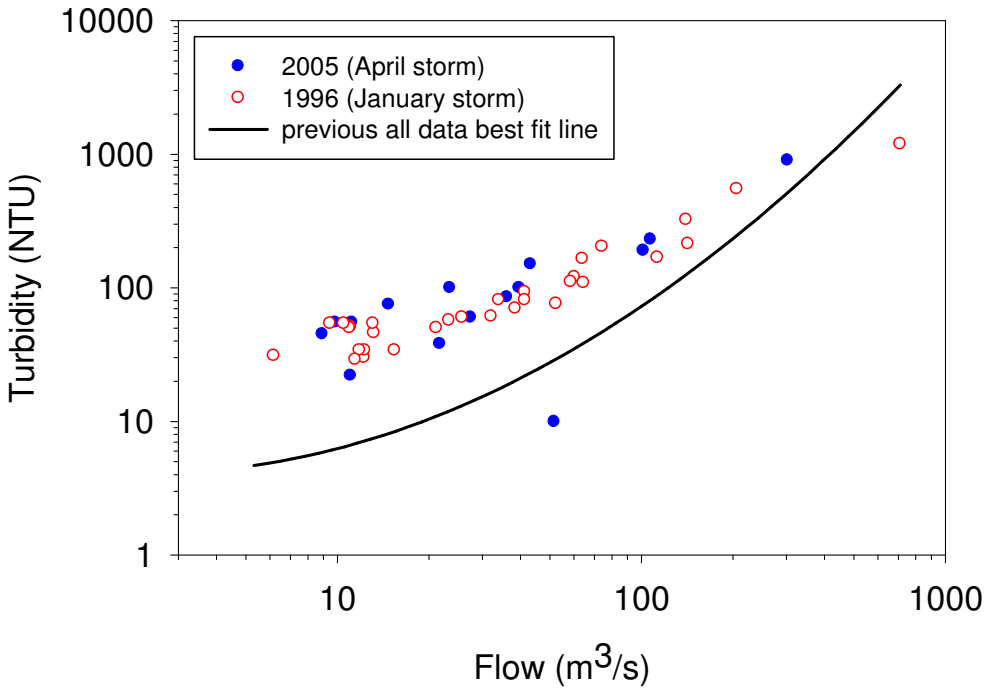

Figure 8. Examples of prolonged elevated turbidity levels at E16i followed by January 1996 and April 2005 runoff events in the Esopus Creek watershed.

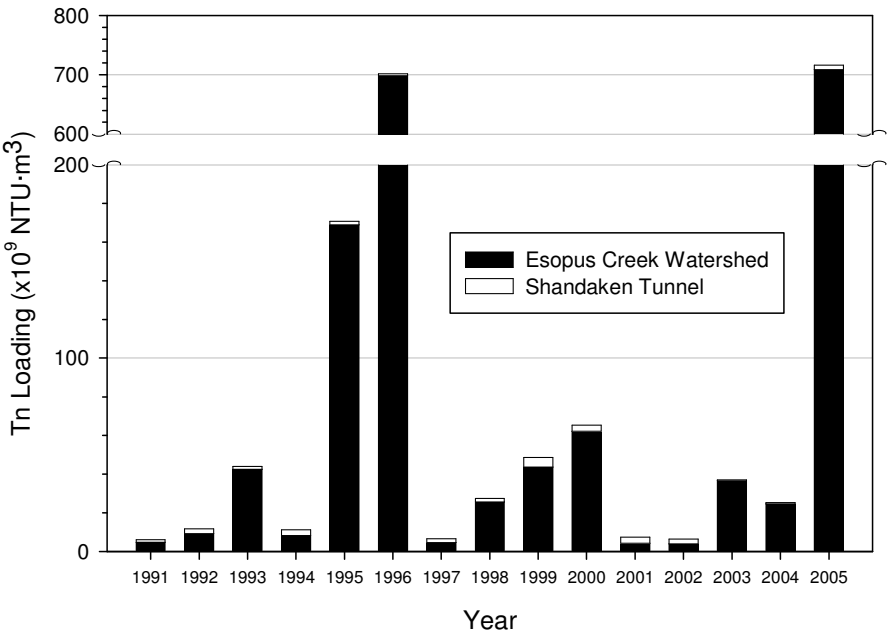

Figure 9. Annual turbidity loading from the Esopus Creek watershed and Shandaken Tunnel for 1991-2005.

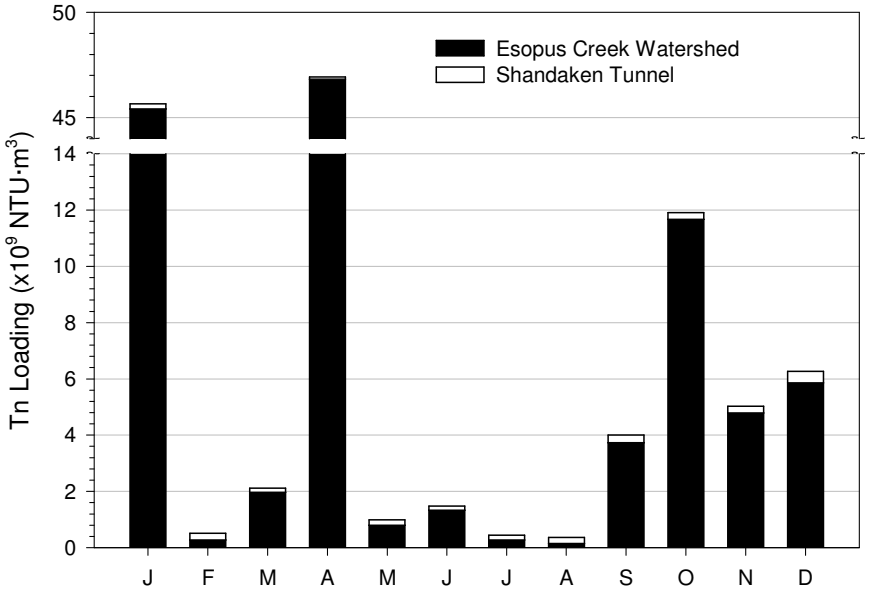

Figure 10. Seasonal variations in turbidity loading from the Esopus Creek watershed and Shandaken Tunnel represented as average of 1991-2005.

To examine seasonality in the turbidity loading, monthly average values were plotted for 1991-2005 (Figure 10). January and April show the largest loading while February and May-August the least. The maximum contribution from the tunnel (60%), relative to the total load, is observed in the low flow period of August (Figure 10). To further resolve the seasonality in the

loading, monthly bar charts were prepared for each of the 1991-2005 years (Figure 11). The turbidity loading scale is varied for each of the years to depict the rather large seasonal variations and the relative contribution of the Shandaken Tunnel (Figure 11). The highest turbidity loading during any single month was observed in January, 1996 and April, 2005; nearly all of it originated from the Esopus Creek watershed (Figure 11).

Table 7. Yearly turbidity loadings from the Esopus watershed and Schoharie Reservoir diversion tunnel for 1991-2005.

Year	Watershed Turbidity Load ($x10^9$ NTU·m^3)	Schoharie Tunnel Turbidity Load ($x10^9$ NTU·m^3)	Schoharie Tunnel Turbidity Load as % of Total Load
1991	4.7	1.2	20.8
1992	9.2	2.5	21.0
1993	42.4	1.5	3.4
1994	8.3	2.9	25.6
1995	169.0	1.9	1.1
1996	699.0	3.4	0.5
1997	4.6	2.0	30.7
1998	25.6	1.8	6.5
1999	43.6	5.1	10.4
2000	62.2	3.1	4.8
2001	4.2	3.1	42.9
2002	3.9	2.5	38.4
2003	36.6	0.4	1.0
2004	24.7	0.6	2.5
2005	708.0	7.6	1.1
1991-2005 Avg	**123.1**	**2.6**	**2.1**

b. Turbidity input to Ashokan Reservoir for 2005:

Despite automated measurements of turbidity at E16i, continuous values were not available in certain intervals of 2005 (total of 82 days) due to instrumentation breakdown. The missing values were estimated from one of the following methods whichever was considered appropriate to the situation: (a) storm-specific flow-turbidity relationship(s) from the partially available measurements (for example, see Figure 12) to estimate missing values during the same storm, (b) flow-turbidity relationship from the available measurements combined for multiple storms when no data are available for another storm (for example, see Figure 13), (c) linear interpolation, (d) use DEP's routine and storm monitoring data. Once all missing turbidity values were estimated, the loads could be computed by multiplying hourly flows with hourly turbidities.

The timeseries of flow and turbidity at various sites for 2005 are shown in Figure 14. Salient features to note are: (i) a huge runoff event in April with Q > 1000 m^3/s [Figure 14(a)]. An event of this magnitude had been documented only once earlier in January 1996 during the study period of 1991-2005. (ii) Seven other large events with Q > 100 m^3/s [Figure 14(a)] occurred in 2005. (iii) Concurrent with these events, the Schoharie Tunnel flow was drastically

reduced [Figure 14(a)]. (iv) Turbidity at E16i was extremely high; often exceeding 100 NTU during these events [Figure 14(b)]. The turbidity at SRR2 was generally less than at E16i and the peak values were associated with very small discharge volumes [Figure 14(b)]. (v) In terms of amount of turbidity, the contribution of Schoharie Tunnel diversion was several orders of magnitude less than that from the watershed during these runoff events [Figure 14(c)]. (vi) The turbidity leaving Ashokan Reservoir remained high for > 2.5 months followed by the April event [Figure 14(d)]. (viii) Catskill Aqueduct effluent was treated with alum for extended interval (77 days) following April-event to reduce turbidity [Figure 14(e)].

The watershed runoff events of April, October, and December 2005 caused elevated levels of turbidity in the water leaving Ashokan Reservoir and triggered three alum treatment events at the CATALUM site before entering Kensico Reservoir (Figure 14(e)). As shown in Table 8, the Shandaken Tunnel's contribution to the total turbidity loading was very small during all of the three runoff events that triggered alum treatment. The total annual turbidity load for 2005 from the watershed as computed from the detailed observations was 2.5×10^{11} NTU·m^3, which is less (68%) than the estimated load from Q-Tn relationship (Figure 7), reflecting variability and uncertainty in the relationship. None the less, the tunnel's contribution remains relatively very small (7.6×10^9 NTU·m^3) in 2005.

Table 8. Turbidity load from Schoharie Tunnel diversion for 2005.

No.	Duration of Events	Turbidity from Shandaken Tunnel during Event (% of Total)
1	3/28 to 4/20	0.01
2	10/7 to 10/28	0.6
3	11/29 to 12/5	4.6

4. Summary

- Shandaken Tunnel contributed 0.5% (3.4 B NTU·m^3) in 1996 to 43% (3.1 B NTU·m^3) in 2001 of total turbidity load to Ashokan Reservoir on an annual basis.
- Average turbidity loading for the study period from the Shandaken Tunnel was 2.1% of the total load.
- Turbidity loading from Esopus Creek ranged from 3.9 B NTU·m^3 in 2002 to 708 B NTU·m^3 in 2005. The rather large range in turbidity loading from the watershed is due to interannual variability in runoff events.
- Highest relative turbidity loading from Shandaken Tunnel most often occurred during low-flow months of February, July and August.
- Turbidity patterns for 2005 at E16i were documented using more temporally detailed monitoring data from installed robotic monitoring units.
- Alum treatment(s) in 2005 at site CATALUM was triggered by elevated turbidity inputs from Esopus Creek.

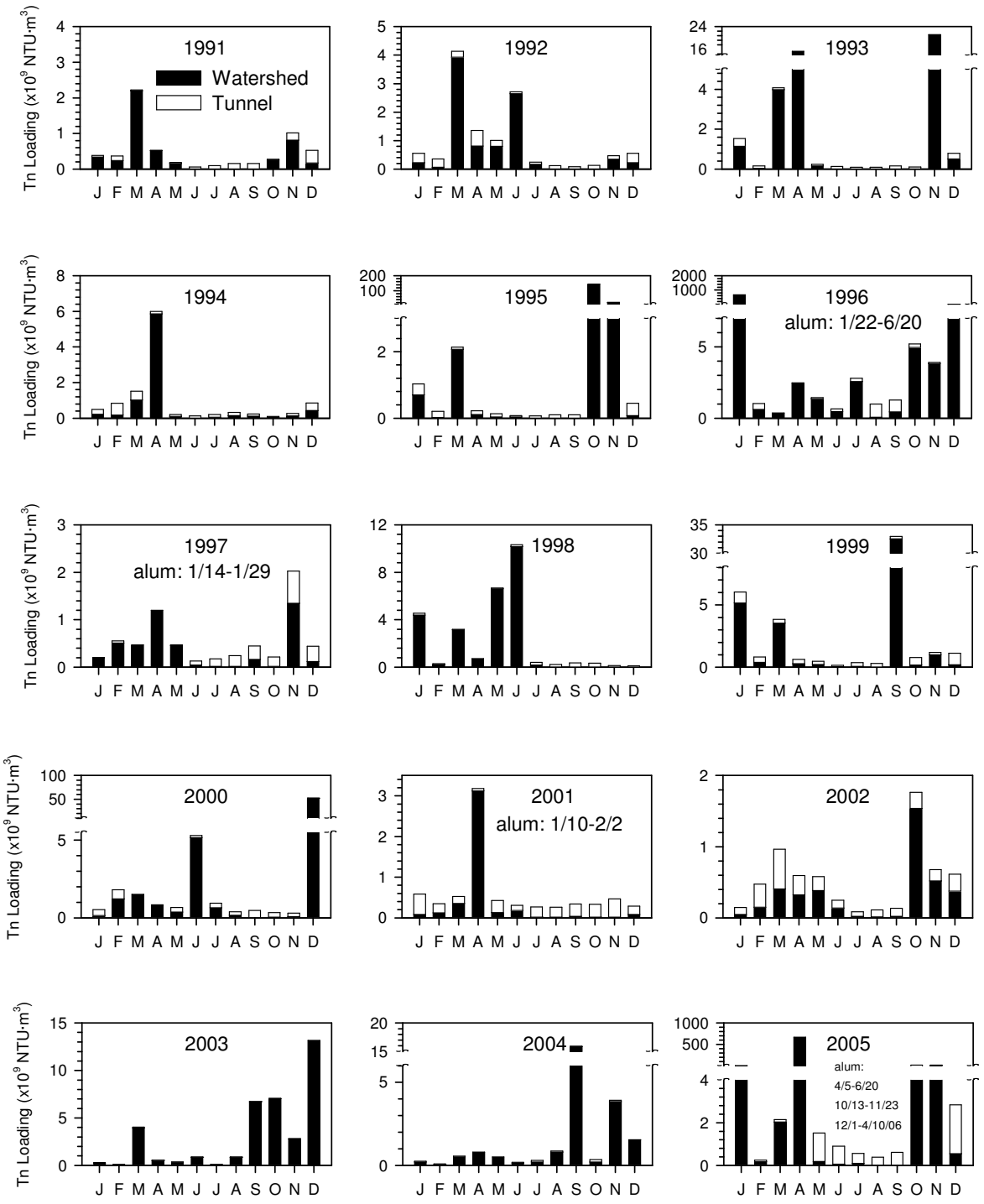

Figure 11. Seasonal distributions of turbidity loading from the Esopus Creek watershed and Schoharie diversion tunnel for 1991-2005.

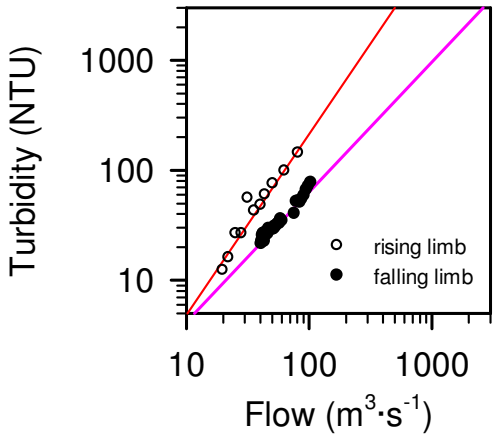

Figure 12. An example of flow-turbidity relationship for the storm event of 1/13/2007-1/17/2007. The rising and falling limbs of the storm hydrograph are regressed separately.

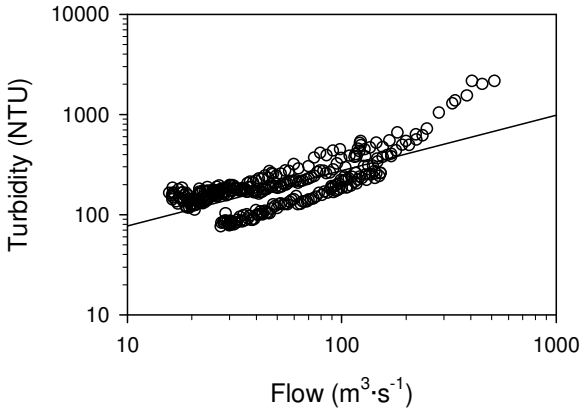

Figure 13. An example of flow-turbidity relationship for the storm event of 10/7/2007-10/16/2007 and 11/30/2007. Only the falling limbs of the storm hydrographs are regressed.

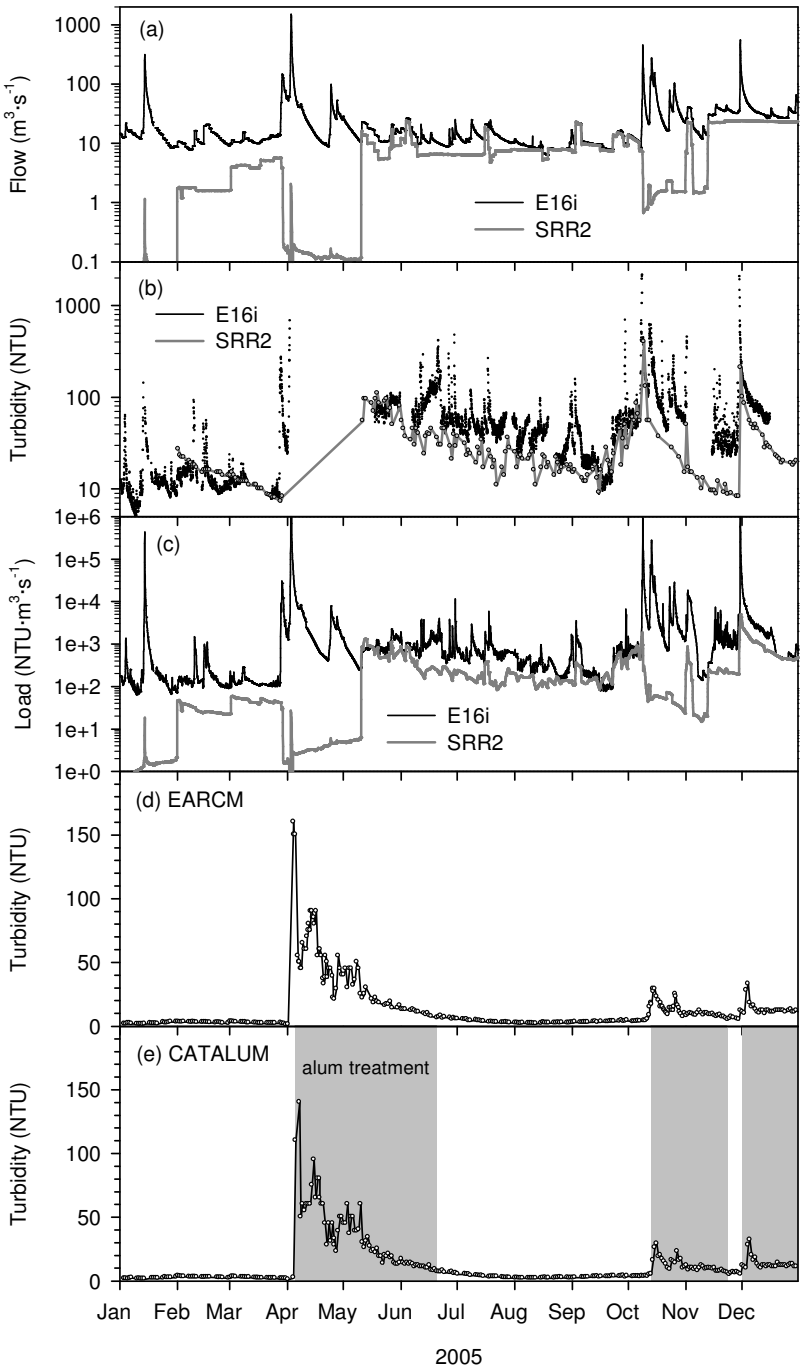

Figure 14. Timeseries of (a) hourly flow at SRR2 and E16i, (b) turbidity (interpolated) at SRR2 and E16i (15-min robohut data), (c) hourly turbidity loads at SRR2 and E16i, (d) turbidity at EARCM site where the water enters in the Catskill Aqueduct, and (e) turbidity at CATALUM site where the water leaves the Catskill Aqueduct. The shaded portion corresponds to days of alum treatment.

C. Turbidity Loading Estimated from Total Suspended Solids Loading (Question 3)

We examined the possibility of using TSS measurements to estimate turbidity loading from the watershed and the tunnel. As compared to turbidity population, substantially smaller population of TSS measurements (Table 9) was available for the study period. While the relationships between TSS and turbidity are reasonable (Figure 15 for site E16i; $r^2 = 0.82$, and Figure 16 for site SRR2; $r^2=0.58$), they are imperfect, as evidenced by the observed scatter (variability in turbidity associated with a given TSS observation). Use of TSS as a metric to assess the turbidity issue for Ashokan Reservoir is possible, but is not necessary for these investigations as the required turbidity data is explicitly available. Moreover, TSS is a systematically flawed metric of light scattering (the issue here is turbidity/light scattering). A major portion of the observed scatter in the TSS versus turbidity relationship is associated with the fundamental differences of the particle size dependencies of TSS (a gravimetric measure) and turbidity (an optical measure).

Table 9. Comparison of populations of turbidity and TSS measurements.

Site	Agency	Counts of Tn	Counts of TSS	Years
E16i	DEP	522	273	1995-2005
	DEP	473	373	1995-2005 (storms)
	UFI	728	11	2005
SRR2	DEP	1812	622	1991-2005

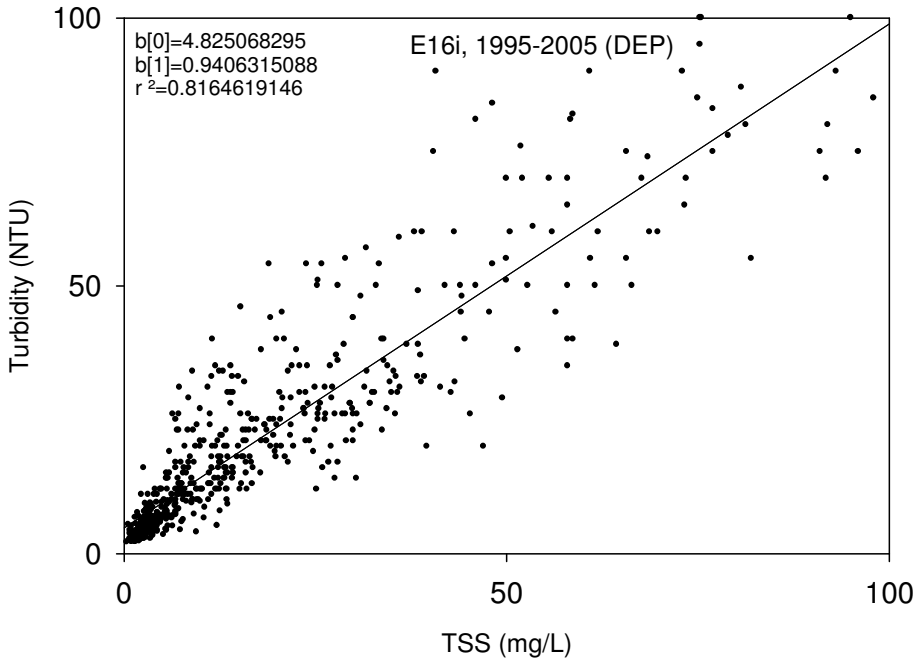

Figure 15. Turbidity-TSS relationship at E16i with 1995-2005 data.

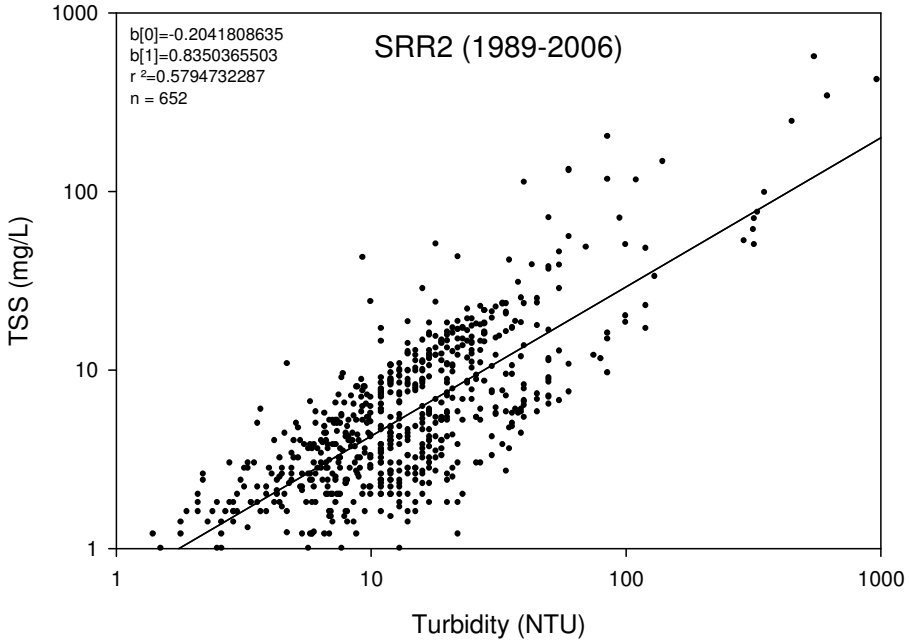

Figure 16. Turbidity-TSS relationship for Shandaken Tunnel discharge at SRR2 with 1989-2006 data.

D. Summary Responses to the Questions of the Watershed Inspector General and Assistant Attorney General

Summary statements for each question are presented below:

1. Question 1
   A sophisticated technology was used to address this question, scanning electron microscopy interfaced with automated x-ray microanalysis and image analysis (SAX). SAX measurements on samples collected from throughout the Catskill System have provided definitive information concerning the extent of differences in the "potency" and persistence of turbidity causing particles from the different portions of the system (particularly Schoharie Reservoir via the Shandaken Tunnel vs. Esopus Creek). The light scattering (i.e., turbidity) features of the particle population, including chemical composition, extent of nonsphericity (e.g., shape), and relative contribution of the particle sizes to turbidity, were found to be highly uniform throughout the system. Specifically, the hypothesis that the turbidity from Schoharie Reservoir is substantially different from, or more problematic than other portions of the Catskill System (e.g., Esopus Creek) is not supported.

2. Question 2
   Detailed loading calculations were conducted based on long-term (1991-2005) monitoring of flow rates and turbidity that partitioned contributions from the Shandaken Tunnel (i.e., Schoharie Reservoir) vs. Esopus Creek (e.g., stream bank deposits). Wide variations in total loading were determined seasonally and year-to-year, with major increases associated with

intervals of elevated runoff. A large fraction of the turbidity received by Ashokan Reservoir has occurred over comparatively small portions of most years during high flow intervals, a widely observed phenomenon for particulate constituents. Esopus Creek has been the dominant source of turbidity to Ashokan Reservoir. The contribution from Shandaken Tunnel was estimated to be only about 2% for the 1991-2005 period. Review of particularly detailed turbidity data sets available for Esopus Creek for 2005, and associated turbidity loading estimates, established that each of the three alum treatments required in that year were "triggered" by inputs from Esopus Creek rather than the Shandaken Tunnel.

3. Question 3
   Use of total suspended solids (TSS) as a surrogate of turbidity to support the development of turbidity loading estimates and partitioning of contributions to the overall load to Ashokan Reservoir is possible but is not necessary as:
   i. the required turbidity data is explicitly available,
   ii. the population of TSS observations for this system is substantially smaller than for turbidity measurements, and
   iii. TSS is a systematically flawed metric of light scattering.

References

Davies-Colley, R. J., W. N. Vant and D. G. Smith. 1993. Colour and Clarity of Natural Waters. Ellis Horwood, New York, New York. 310 p.

Davies-Colley, R. J., and D. G. Smith. 2001. Turbidity, suspended sediment, and water clarity: A review. J. Am. Water Resour. Assoc. **37:** 1085–1102.

O'Donnell, D. M., and S. W. Effler. 2006. Resolution of impacts of runoff events on a water supply reservoir with a robotic monitoring network. J. Am. Water Resour. Assoc. **42:** 323–336.

Peng, F., and S. W. Effler. 2007. Suspended minerogenic particles in a reservoir: Light scattering features from individual particle analysis. Limnol. Oceangr. **52(1)**: 204–216.

Peng, F., D. L. Johnson, and S. W. Effler. 2002. Suspensoids in New York city's drinking water reservoirs: Turbidity apportionment. J. Am. Water Resour. Assoc. **38:** 1453–1465.